



The foehn wind east of the Andes in a 20-year climate simulation

Pablo Luis Antico^{1,2} · Sin Chan Chou³ · Claudio Antonio Brunini^{1,2}

Received: 22 January 2019 / Accepted: 9 June 2020 / Published online: 20 June 2020
© Springer-Verlag GmbH Austria, part of Springer Nature 2020

Abstract

This study investigates the spatial structure and the seasonal occurrence of foehn wind to the east of the Andes using a flow blocking analysis in a 20-year climate simulation. The latter was performed by the Eta-CPTec regional model at 50-km horizontal resolution. This version of the model includes a cut-cell scheme to represent topography and a finite-volume vertical advection scheme for dynamic variables. The results indicate that foehn wind more frequently blows during winter and spring on the eastern slopes of the Andes, except to the south of 37° S where it blows at all seasons. Higher mountains of the Central Andes (27° S–35° S) and the High Plateau (15° S–27° S) result in blocked foehn events, with a weak adjustment to the geostrophic balance. On the Central Andes, rain and snow on mountain tops may also contribute to generate foehn wind on the eastern slopes. The results show that a low pressure develops to the east of the Central Andes, and also to the east of the High Plateau when foehn blows. Lower mountains in Patagonia (to the south of 37° S) result in more frequent non-blocked foehn event, with better adjustment to the geostrophic balance.

1 Introduction

The term foehn refers to the downslope warm and dry wind that blows on the leeside of mountains (Brinkmann 1971). Even though the term is worldwide used, it locally received different names. This is the case, for instance of the *zonda* wind in South America, the wind that blows along the eastern slopes of the Andes mountains. In addition to the sudden increase in temperature and the reduction in relative humidity, it is usually accompanied by strong gusts (Norte 2015). The most severe events seriously affect activities in many towns to the east of the Andes, causing damages in power lines, constructions, fires, air traffic disruption among

other problems (Norte 1988, 2015; Norte et al. 2008). The term *zonda* arises from the way that local inhabitants in the Andean valleys and the lowlands to the east referred to it in the province of San Juan, Argentina, around 31° S. However, according to Schwerdtfeger (1976), downslope winds with similar characteristics as the *zonda* also blow in other valleys east of the Andes between 33° S and 15° S. But the Andes mountains undergo changes of characteristics along this range of latitudes (Fig. 1). The *Central Andes* extend from 27° S to 35° S where the crest of the main mountain range is about 3000 m with higher peaks, where the Aconcagua with its 6959 m is the highest peak in South America. To the north of 27° S, the Andes become wider with a *High Plateau* (about 4000 m). Between the latitude 35° S and 37° S, the crest of the main mountain range descends from 3000 to 2300 m. To the south of 37° S, the Andes extend to the southern tip of the continent. The *Patagonia* extends from the Andes to the Atlantic Ocean, rising in terrace fashion from coastal cliffs to the base of the Andes. This tableland region rises to an altitude of 1500 m, sometimes similar to the main mountain range of the Andes. Even though there is no reference in the literature about foehn wind at Patagonia tableland, strong and dry westerly winds are well known to blow in the area.

Zonda to the east of the Central Andes has been the subject of several studies. Norte (1988) obtained the first climatology of the *zonda* at Mendoza using observations from

Responsible Editor: F. Mesinger.

✉ Pablo Luis Antico
pablo.antico@aggo-conicet.gob.ar

¹ Argentinean-German Geodetic Observatory, Consejo Nacional de Investigaciones Científicas y Técnicas, Camino Gral. Belgrano km 40, Berazategui, Provincia de Buenos Aires, Argentina

² Facultad de Ciencias Astronómicas y Geofísicas, Universidad Nacional de La Plata, Paseo del Bosque s/n, B1900FWA, La Plata, Provincia de Buenos Aires, Argentina

³ Instituto Nacional de Pesquisas Espaciais (INPE), Rod. Pres. Dutra, km 39, Cachoeira Paulista, SP 12630-000, Brazil

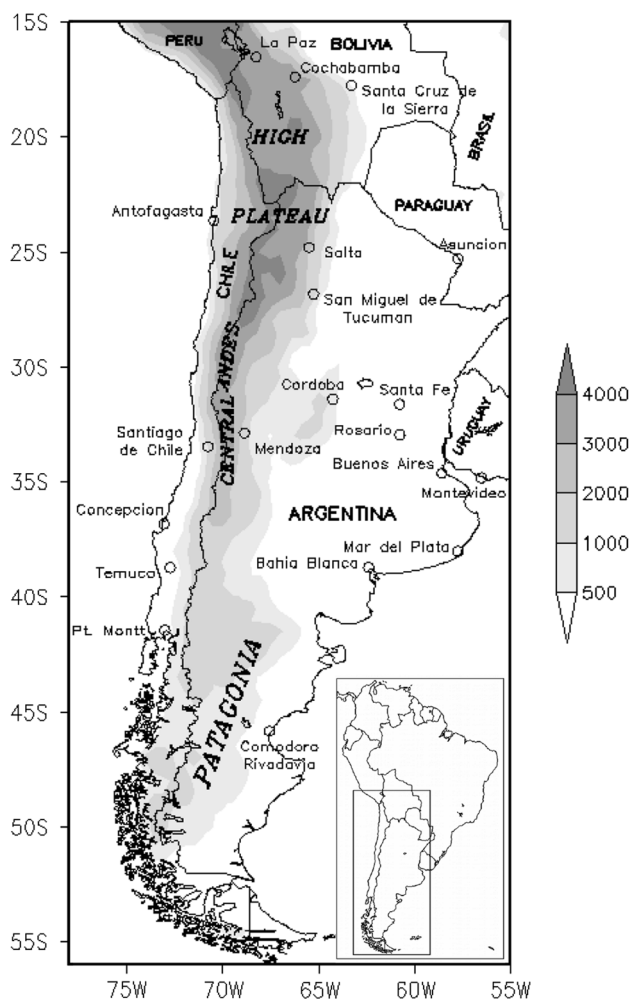


Fig. 1 The Andes mountain range as seen by the Eta-CPTEC model in the 20-year climate simulation. Shades in meters

ground stations and radiosondes. In his study, Norte (1988) classifies the zonda as high zonda and surface zonda, according to the elevation of the sites where the zonda blows. Seluchi et al. (2003) used the zonda classification of Norte (1988) to simulate particular cases of zonda events with the Eta model. They compared their results with observations and proposed some explanations for the physical processes involved in each type of zonda. A numerical simulation of a severe case of zonda wind was performed by Norte et al. (2008) with the BRAMS model (the Brazilian version of the RAMS model). Their results showed the ability of the model to capture the main features of this particular event. Later, the same case of severe zonda was analyzed in a forecast experiment with the Eta model, using a version of the so-called ‘cut-cell’ discretization of topography (Mesinger et al. 2012; Mesinger and Veljovic 2017). Those results highlighted the performance achievable using the eta coordinate with its cut-cell formulation to simulate the foehn in the case of complex topography with steep slopes as in the

case of the Central Andes. Puliafito et al. (2015) performed a numerical simulation with the WRF model to reproduce the main features of two events of zonda wind at Mendoza.

In addition to the aforementioned case studies, Antico et al. (2017) obtained a climatology of zonda wind occurrence near Mendoza from a 20-year climate simulation with the Eta-CPTEC model. There is a lack of studies that investigate the foehn to the east of the Andes outside the Central Andes region. To the west of the Central Andes, the foehn wind is locally known as *raco* wind, and to the west of Patagonia it is known as *puelche* wind (Rutlant and Garreaud 2004). Montecinos et al. (2017) made a climatic characterization of the puelche wind along a latitudinal range to the west of the Andes using climate forecast system reanalysis (CFSR) at 0.5° of horizontal resolution.

Because the term zonda is usually reserved for the foehn to the east of the Central Andes, we adopt the more general expression *foehn* to refer to these winds at any latitude south of 15° S along the eastern slopes of the Andes. The objective of this study is to investigate the foehn wind to the east of the Andes using results from a 20-year climate simulation. The foehn is characterized for different Andean regions in terms of synoptic scale features of the atmospheric circulation. The blocking flow to the west of the Andes is analyzed. Then, the vertical structure of the foehn wind is characterized at different latitudes.

2 Data and methodology

Data used for foehn detection come from a 20-year climate simulation described in Antico et al. (2017) for the period 1989–2008. This simulation was produced using the Eta-CPTEC regional model at 50-km horizontal resolution and 38 vertical levels. The frequency of model output was 6 h. A spin-up of 1 year was used to allow coupling between the atmosphere and the soil conditions, then this first year of model integration was discarded. Lateral boundary conditions were taken from the ERA-Interim global reanalysis at 150-km horizontal resolution and every 6 h (Dee et al. 2011). Sea surface temperature reanalysis was updated on a daily basis. Lower boundary conditions were provided by the four-layer NOAH soil model (Chen et al. 1997; Ek et al. 2003). Cumulus parameterization was given by the Betts–Miller scheme modified by Janjić (1994), and cloud microphysics by the Zhao scheme (Zhao et al. 1997). The Monin–Obukhov similarity was used in the surface layer with Paulson stability functions coupled to molecular sub-layer over land and ice (Zilitinkevich 1995) and over water (Janjić 1994). Form drag scheme dependent on wind direction (Mesinger et al. 1996) was applied. Parameterization of turbulence above the surface layer was represented by the Mellor–Yamada 2.5 closure scheme (Mellor and Yamada

1982) with various refinements (see Janjić 1990, 2002; Mesinger 1993, 2010).

A particular feature of the Eta model is the so-called ‘sloping-steps’ refinement of the eta discretization (Mesinger et al. 2012). This discretization is a simple version of what is generally referred to as a cut-cell scheme for the representation of topography. Another special feature is the van Leer-type finite-volume vertical advection of all dynamic variables (Mesinger and Jovic 2002).

To detect foehn wind in the climate simulation, we propose a criterion based on the simultaneous occurrence of downslope wind, positive anomalies of air temperature, and negative anomalies of relative humidity. The criterion uses near surface variables, such as wind at 10 m, temperature and relative humidity at 2 m above ground. Downslope wind is considered as detected when surface wind blows against the terrain elevation gradient. Surface temperature anomaly is defined as the difference between current surface temperature and the corresponding long-term monthly mean for each specific hour, i.e. 00, 06, 12, and 18 UTC. Mean values are obtained as an average over the entire simulated period. Similar definition is formulated for the relative humidity anomaly. A lower limit is defined for the slope of the terrain elevation to filter out very small slopes, whereas a threshold of 4 m s^{-1} is adopted for wind velocity to filter out light breezes. Positive temperature anomalies greater than one standard deviation and negative relative humidity anomalies less than one standard deviation have been defined as thresholds for foehn detection. These thresholds permit to filter out cases with light anomalies of temperature and relative humidity.

The methodology to detect foehn wind is applied to each grid box to the south of 15° S along the main mountain range of the Andes. The resulting spatial frequency distribution of the number of foehn events per year is shown in Fig. 2. Within each region of the Andes shown in Fig. 1, at least one grid point is selected where the relative maximum of foehn frequency is detected.

3 Results

The methodology applied to detect foehn wind in the 20-year climate simulation reveals that foehn occurs on both sides of the Andes, as shown in Fig. 2. However, the higher frequencies are on the eastern mountain slopes. In general, the foehn becomes more frequent as the terrain elevation increases from the lowlands on the east to the mountain crest on the west. The highest foehn frequencies with more than 140 cases per year occur to the east of the Central Andes and to the east of the High Plateau. This is the case for the absolute maximum greater than 200 cases per year on the far eastern slopes in Bolivia to the north of 22° S . But this maximum

FOEHN OCCURENCE PER YEAR (1990–2008)

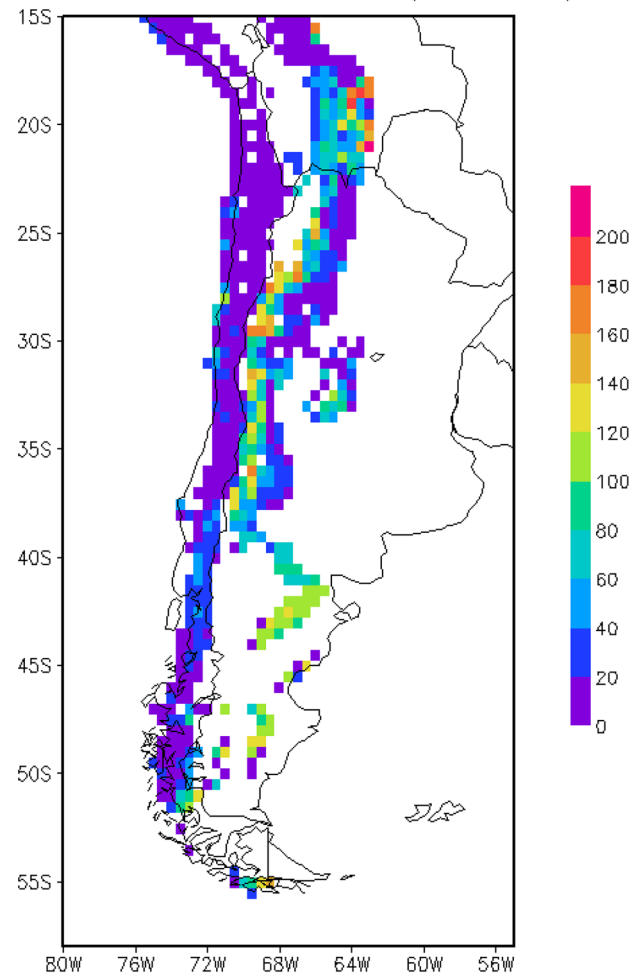


Fig. 2 Detection of foehn in the 20-year climate simulation. Units are number of events per year

does not result from air flow crossing the Andes, as discussed in a further section. To the south of 38° S , wide plateaus separate the crest of the Andes from the eastern slopes where the foehn wind is detected. This situation explains the gap in the foehn occurrence in the middle of Patagonia.

It is noteworthy that foehn is also detected in the low mountains to the east of the Central Andes near the city of Cordoba, Argentina. On the southern coast of the Tierra del Fuego Island, to the south of the continent, the foehn is also detected.

In the following subsections, we investigate the foehn occurrence at different regions along the eastern slopes of the Andes to the south of 15° S . Composite analysis is performed when foehn blows at selected points within each region. These grid points are chosen because they exhibit the highest foehn event frequency in a given region, as seen in Fig. 2. The corresponding grid points for each region are listed in Table 1. Composites consist of mean fields of

Table 1 Brunt-Väisälä frequency (N) and non-dimensional mountain height (h) at the three Andean regions when maximum foehn frequency occurs

| Z (m) | P (hPa) | N (10^{-2} s^{-1}) | h |
|---|-----------|----------------------------------|------|
| Central Andes (31.5° S 68.5° W)—July $h_0 = 3600 \text{ m}$, $n = 211$, $U = 17 \text{ m s}^{-1}$ | | | |
| 3000 | 700 | 1.06 | 0.44 |
| 2500 | 750 | 1.19 | 0.84 |
| 2000 | 800 | 1.29 | 1.36 |
| High Plateau (25.0° S 65.5° W)—June $h_0 = 4100 \text{ m}$, $n = 193$, $U = 15 \text{ m s}^{-1}$ | | | |
| 3600 | 650 | 1.17 | 0.47 |
| 3000 | 700 | 1.19 | 0.95 |
| 2500 | 750 | 1.26 | 1.43 |
| Patagonia (48.5° S 69.0° W)—September $h_0 = 1400 \text{ m}$, $n = 254$, $U = 10 \text{ m s}^{-1}$ | | | |
| 1000 | 900 | 1.18 | 0.59 |
| 750 | 925 | 1.16 | 0.87 |
| 100 | 1000 | 1.11 | 1.55 |

The location of the reference point (latitude and longitude), the month with the maximum foehn frequency, the relative height of the mountain crest (h_0), the number of foehn cases (n) and the velocity of the wind perpendicular to the mountain at the crest level (U) are indicated for each region. Values of N and h are listed for three different altitudes (Z) with their corresponding pressure (P)

selected meteorological variables and vertical cross sections perpendicular to the mountain crest. Only those composites with the highest monthly frequency are shown. Monthly frequencies of foehn at each one of the selected grid points are shown in Fig. 3a–c. Composites of surface wind, temperature anomalies, and relative humidity anomalies are shown in Fig. 4a–c, and composites of mean sea level pressure, total precipitation, and snow are shown in Fig. 5a–c.

3.1 Central Andes

The foehn is more frequent during winter with slightly higher frequencies during spring than autumn on the eastern slopes of the Central Andes (Fig. 3a).

The strongest surface winds blow along the eastern slopes of the mountain crest when the foehn occurs at the grid point shown in Fig. 4a.

Positive anomalies of surface air temperature greater than two times the standard deviation occur downslope to the east of the Central Andes. The largest anomalies are found along the same latitude where the strongest surface winds blow on the mountain crest. Positive surface temperature anomalies due to foehn warming spread far to the east over the central mountains of Argentina. Anomalies of relative humidity are consistent with the temperature anomalies, with the lowest values below -2.5 times the standard deviation in the same area where higher temperature anomalies occur.

Precipitation over the western slopes of the Central Andes (Fig. 5a) is also a typical feature when zonda blows in Mendoza (Norte 2015), in the eastern slopes of the Andes. At higher elevations and over the mountain crest, snow may represent more than 50% of the total precipitation (Fig. 5a).

An intense zonal gradient of sea level pressure (SLP) develops across the Central Andes (Fig. 5a). This gradient results from the pressure difference between the high pressures over the Pacific Ocean and the trough to the east of the Andes. The latter, known as northwestern Argentinean low (NAL) (Escobar and Seluchi 2012), typically develops when the zonda blows in Mendoza (Lichtenstein 1980; Seluchi et al. 2003).

3.2 The High Plateau

The annual distribution of foehn occurrence at the eastern slopes of the High Plateau is similar to that of the Central Andes, despite the maximum frequency occurs in June instead of July (Fig. 3b).

The surface wind pattern when foehn blows at the eastern slopes of the High Plateau shows the strongest winds between 25° S and 31° S to the east of the mountain crest (Fig. 4b). The northerly winds that blow east of the Andes over Bolivia and Paraguay result from the deepening of a low pressure as it is discussed latter.

A large area of positive temperature anomalies exceeding 2.5 times the standard deviation, extends along the eastern slopes of the High Plateau, over the reference grid point. Relative humidity anomalies, that reach -2.5 times the standard deviations, are in agreement with the positive temperature anomalies on the eastern slopes. Simultaneously, an area of positive relative humidity anomalies, greater than two times the standard deviation develops along the western Andean slopes between 27° S and 37° S.

There is no precipitation on the western slopes of the High Plateau when the foehn wind blows on the eastern slopes except for some snow around 27° S (Fig. 5b). Precipitation over the western slopes only occurs around the Central Andes, where the latitudes are relatively lower.

Similar to the case of the Central Andes foehn, an intense zonal gradient of SLP develops across the High Plateau (Fig. 5b). This gradient results from the pressure difference between the high pressure over the Pacific Ocean and the low pressure to the east of the High Plateau. This low pressure should not be confused with the Chaco Low, which is a feature of the low-level circulation during summer as part of the South America monsoonal system. Instead, the low pressure in Fig. 5b is a feature of low-level circulation related to the foehn event on the eastern slopes of the High Plateau. Thus, it may be regarded as the northernmost position of the NAL (Escobar and Seluchi 2012) when the foehn wind blows at these latitudes.

Fig. 3 Annual distribution of foehn occurrence on the eastern slopes of the Central Andes (31.5° S 68.5° W) (a); the High Plateau (25.0° S 65.5° W) (b); Patagonia (48.5° S 69.0° W) (c). Vertical axis indicates number of events per month

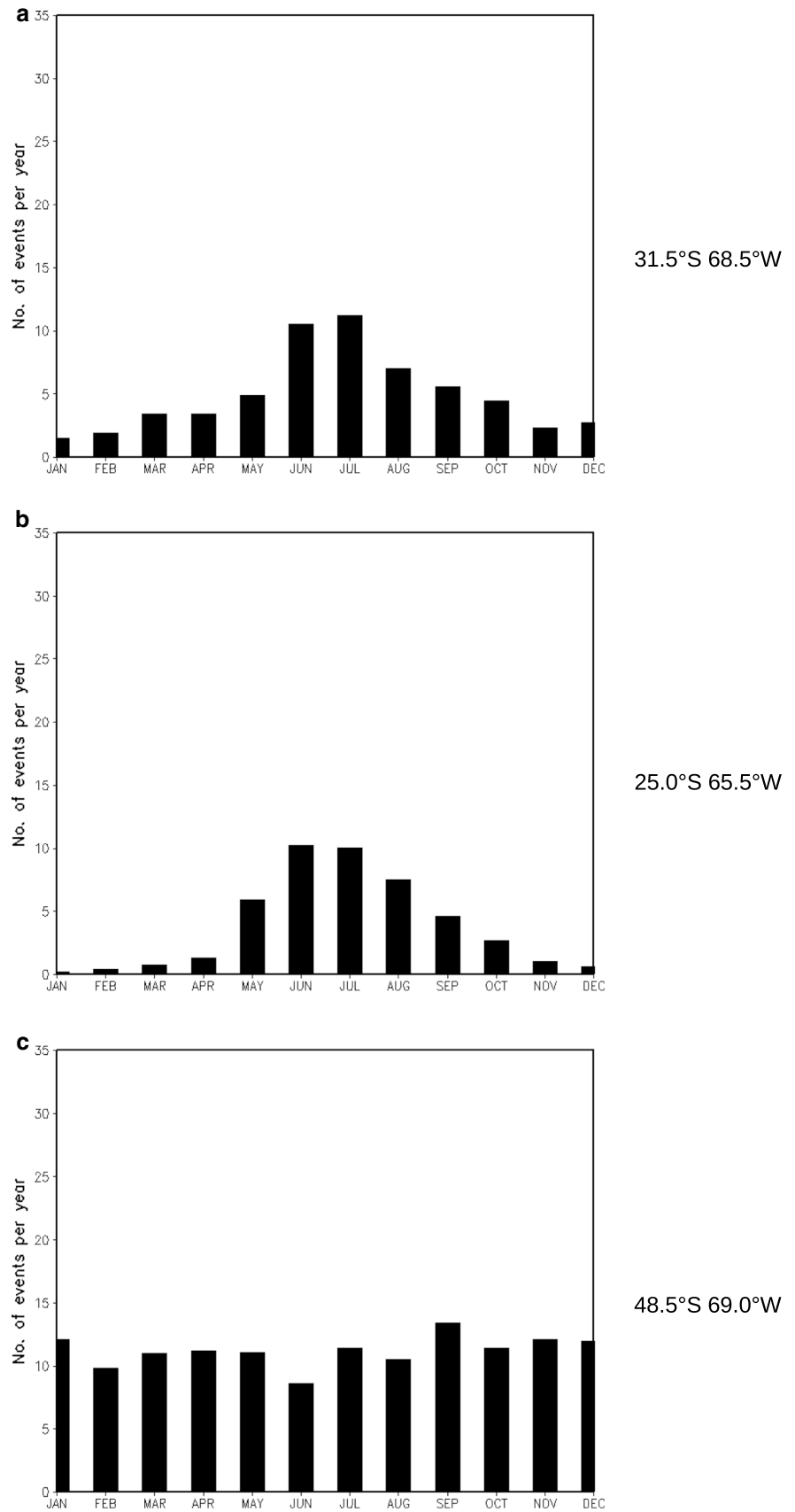


Fig. 4 Composites of surface wind (m s^{-1}) (left column), anomalies of surface temperature (in standard deviations) (middle column), and anomalies of relative humidity (in standard deviations) (right column) for the Central Andes in July (**a**), the High Plateau in June (**b**) and Patagonia in September (**c**). Contours are terrain elevation in meters. Dots indicate the location of the reference point in each region (see Table 1)

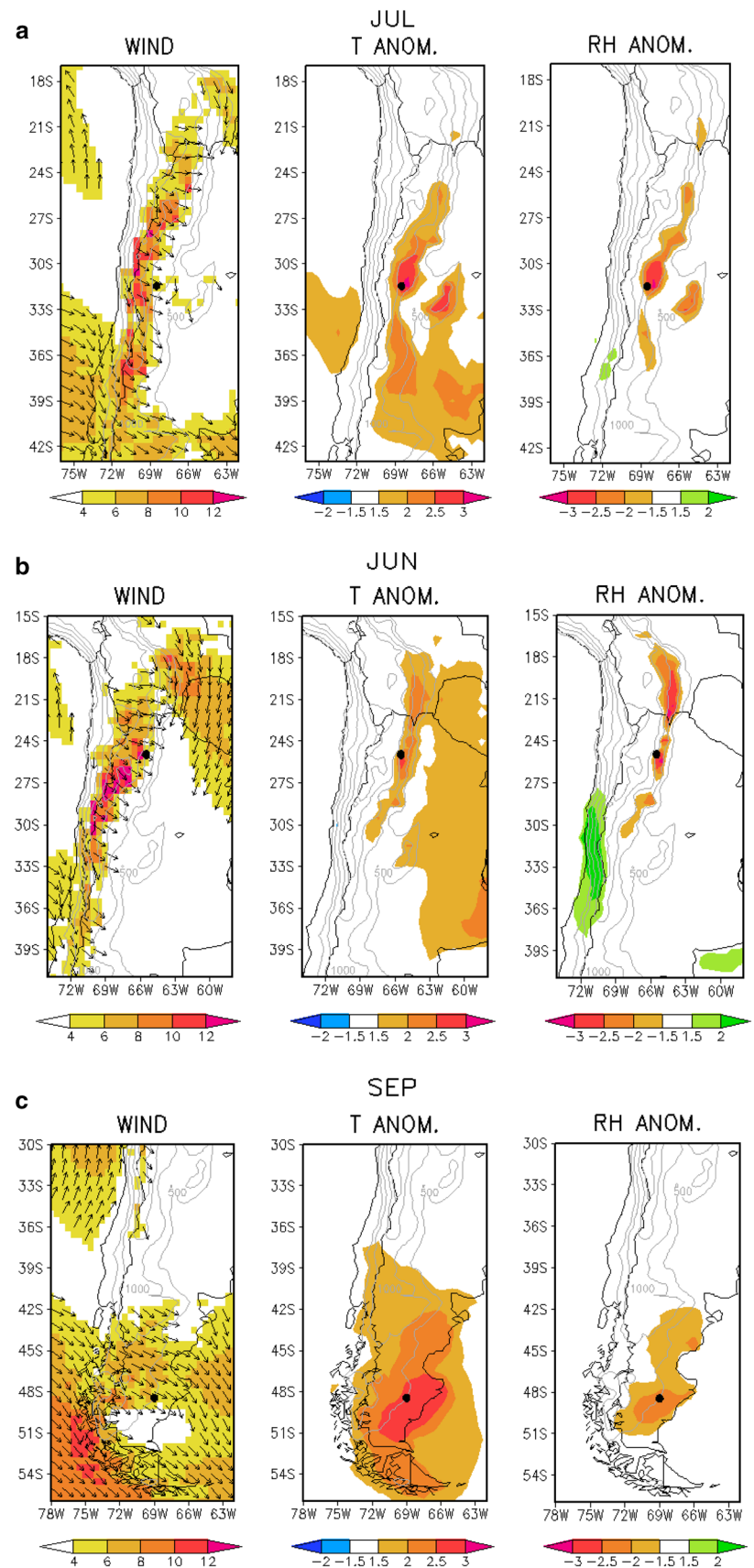
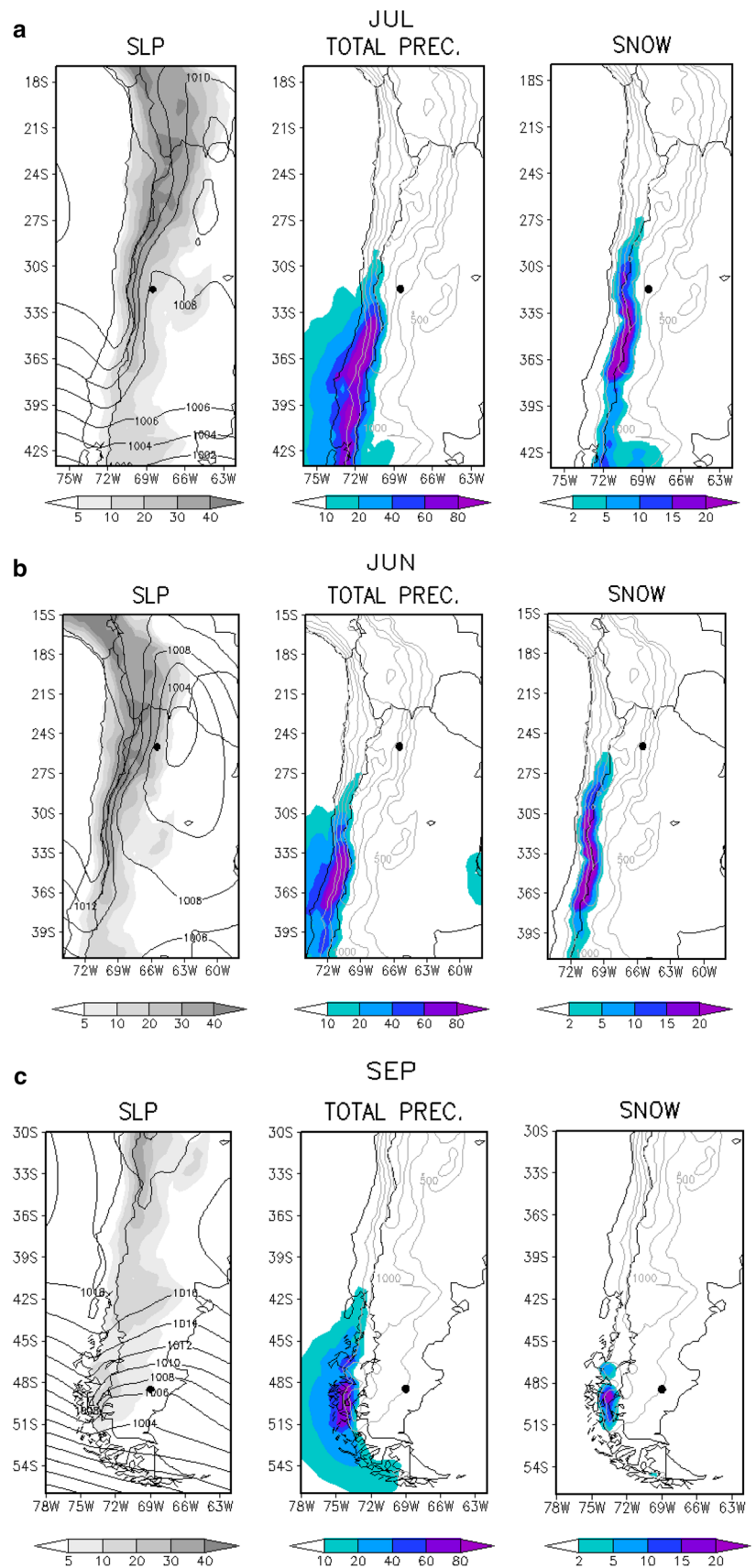


Fig. 5 Composites of total precipitation (mm/day) (middle column), snow (mm/day) (right column) and sea level pressure (in hPa) (left column) for the Central Andes in July (**a**), the High Plateau in June (**b**) and Patagonia in September (**c**). Contours are terrain elevation in meters (shaded in the left column). Dots indicate the location of the reference point in each region (see Table 1)



3.3 Patagonia

The foehn wind on the eastern slopes of Patagonia may occur throughout year, but more frequently in September (Fig. 3c).

Stronger surface winds blow at higher terrain elevations, both on the Andes mountains crest and on the Patagonian plateau to the east (Fig. 4c). The highest wind speeds found over the southwestern coast of the continent result from the intense pressure gradient (Fig. 5c).

Positive temperature anomalies, which exceed 2.5 times the standard deviation, extend all over the Patagonia and spreads downslope to the east of the reference grid point (Fig. 4c). Consistently, minimum anomalies of relative humidity, less than -2 times the standard deviation occur in the same area.

Precipitation occurs upwind of the main mountain range along the Patagonian Andes. The maximum precipitation values are found on the western slopes of the Andes almost at the same latitude of the reference grid point. Figure 5c reveals that approximately 25% of this precipitation is snow.

Figure 5c shows the SLP pattern with a ridge to the west and a trough to the east of Patagonia; however, this pattern is not as an intense cross-mountain pressure gradient as in the case of the other Andean regions.

4 Vertical structure of the atmosphere

To gain insight of the vertical structure of the atmosphere when the foehn blows at the eastern slopes of the Andes, we perform an analysis of vertical sections across the mountains at the latitudes of the reference points in Table 1. These vertical cross sections are obtained from the composites previously discussed in Sect. 3. For each Andean region, the corresponding composites of potential temperature, zonal wind, and vertical motion are shown in Figs. 6a–c, 7a–c and 8a–c, respectively. We assume adiabatic flow, so that the isentropes may be regarded as mean streamlines that describe the flow around the mountains. This flow may pass over the mountains or become blocked, as it is further discussed. The zonal wind represents mostly the wind component perpendicular to the main mountain crest. This is the case for the Andes Mountains at the selected latitudes.

The steep slopes of the Central Andes (Fig. 6a) act as barriers for the westerly flow. The analysis of the isentropes suggests that the low-level flow over the Pacific Ocean is blocked. On the other hand, the flow near the mountain crest overpasses the mountains. On the lee side, isentropes increase their slope as they follow the terrain slope. This indicates that the upper air is descending downslope, but the depth of this downward motion is bounded by a strongly stratified layer beneath the 850-hPa level to the east of the Andes. Above this layer, subsiding air is diverted to the east up to the lower mountains in central Argentina. The vertical cross section of zonal wind (Fig. 7a) shows the increase in wind speed on the lee of the Andes where downward motion

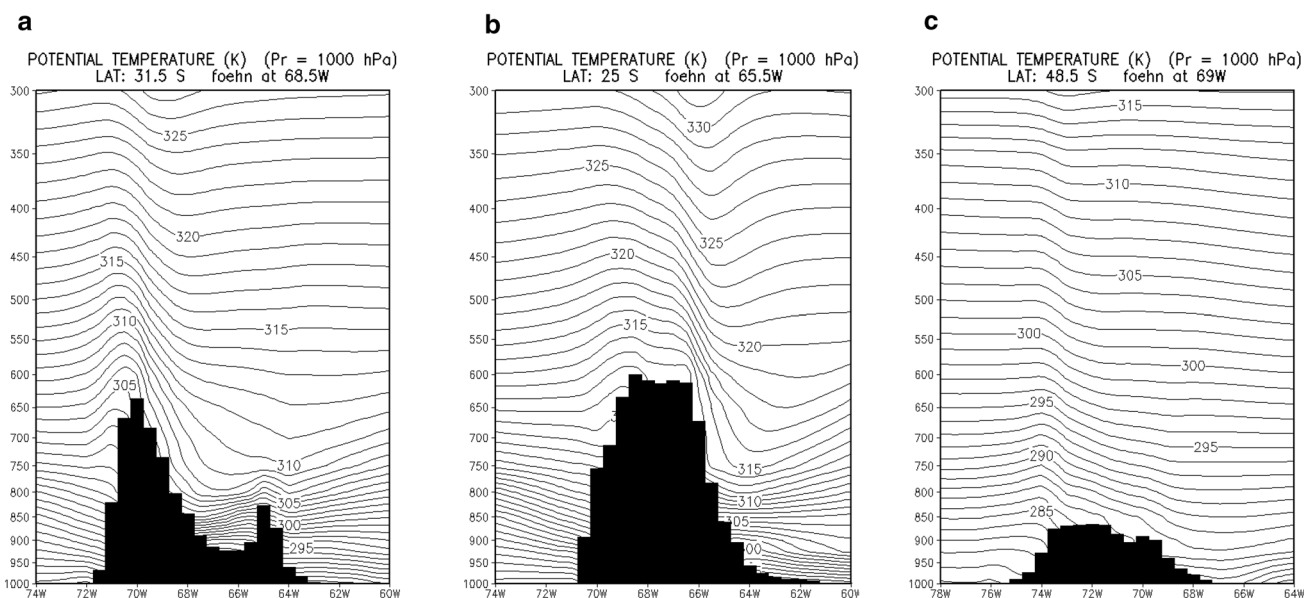


Fig. 6 Vertical cross sections with composites of potential temperature (K) at the latitude of the reference points of the Central Andes in July (**a**), the High Plateau in June (**b**) and Patagonia in September (**c**)

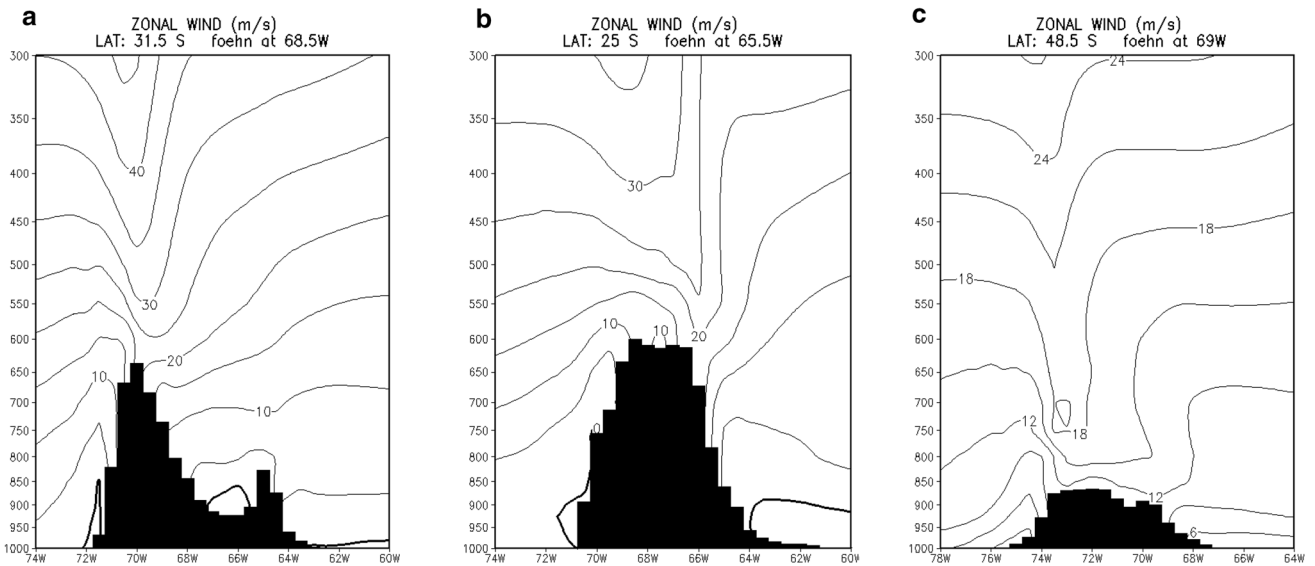


Fig. 7 Same as in Fig. 6 but for zonal wind (m s^{-1}). Thick contour denotes the zero line

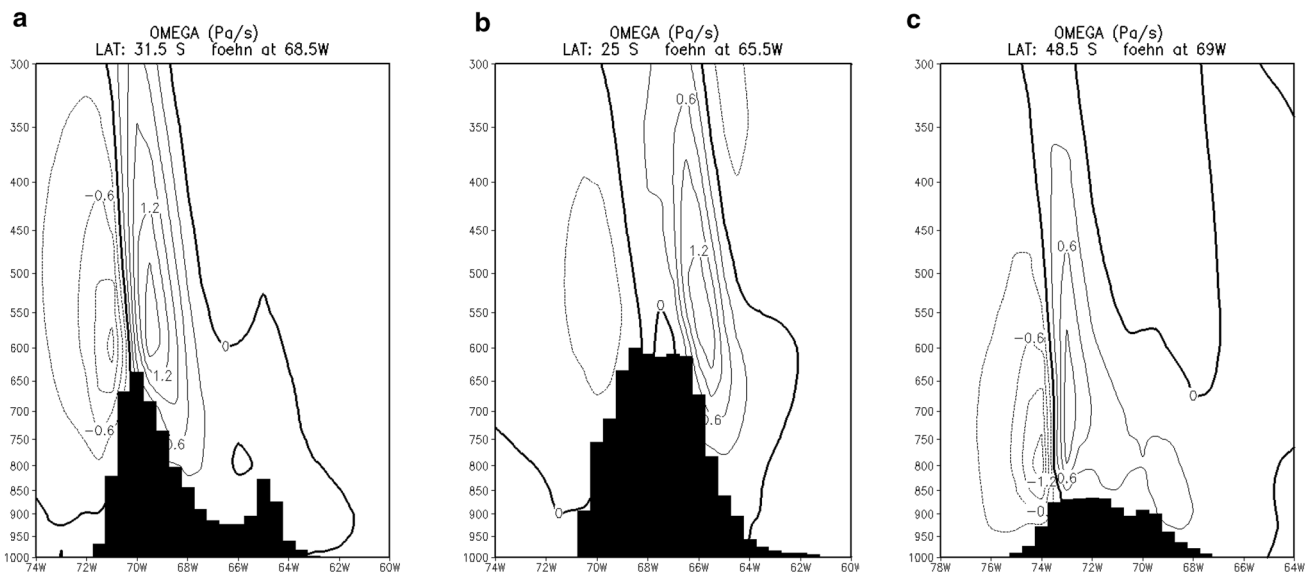


Fig. 8 Same as in Fig. 6 but for vertical motion (Pa s^{-1}). Thick contour denotes the zero line

also occurs (Fig. 8a). Downward transport of zonal momentum occurs to the east of the mountain crest, as the combination of the Figs. 7a and 8a show. Calm winds occur within the stratified layer beneath the 850-hPa level. Similar situation, but to a lesser extent, occurs to the east of the lower mountains in central Argentina at 65°W .

As in the Central Andes, the low-level flow from the Pacific Ocean is blocked by the Andean High Plateau, but the upper level flow crosses the mountain near the 600-hPa level. On the lee of the mountain, the steep slopes of the isentropes indicate subsidence of the upper air. This

downward motion is bounded by the top of a stable layer to the east of the Andes at the 800-hPa level. Downward transport of zonal momentum along the eastern slopes may be inferred by combining the vertical cross sections of the zonal wind (Fig. 7b) and of the vertical motion (Fig. 8b).

Despite the lower elevation, the Patagonian plateau (Fig. 6c) still blocks the low-level flow to the west of the Andes below the 900-hPa level. However, only the air flow at the crest level crosses the mountain and descends along the eastern slopes. Vertical cross section of zonal wind (Fig. 7c) shows a well-defined maximum above the

mountain crest that spans over the Patagonian plateau to the east (Fig. 8c).

The previous analysis of vertical cross sections suggests that part of the impinging flow is blocked by the mountain. This partial blocking of the upwind flow leads to a foehn classification into blocked or non-blocked foehn. Beusch et al. (2017) applied this classification to the foehn on the western slopes of the Andes, somewhat similar to the one applied by Würsch and Sprenger (2015) to the foehn in the Alps. They found that both types of foehn occur to the west of the Andes depending on the latitude and consequently on the mountain height.

To determine the height under which the flow is orographically blocked in our study, we use a non-dimensional mountain height according to the theory of Smith (1988) (see Appendix A). Table 1 shows the resulting values for each of the Andean regions. The lowest level of each region with h greater than unity represents the maximum height under which the impinging flow cannot overpass the mountain. We will refer to it as the *blocking level* above which the flow overpasses the mountain. The blocking level rises as the mountain crest increase, from 2000 m in the Central Andes to 2500 m in the High Plateau. This increase of h results from the increase of h_0 , the relative mountain height, since U , the mean zonal wind, and N , the Brunt–Väisälä frequency remain almost the same in both regions. In Patagonia, the low blocking level results from lower h_0 and to a lesser extent, from weaker U .

As stated by the theory of Smith (1988), the condition for flow collapse onto the mountain lee slopes depends on the values of h . It may be inferred from the results showed in Table 1, that the air flow of the layer immediately above the blocking level fulfills this condition in the three Andean regions. Hence, the downslope wind on the lee slope originates from the upper layers.

According to the same theory, low values of h at higher elevations indicate that air flow may overpass the mountain. This is the case for the highest levels with h less than $\frac{1}{2}$ listed in Table 1 in the Central Andes and the High Plateau. We will refer to it as the *free overpassing level* above which the flow overpasses the mountain without streamline collapse on the lee slope. The free overpassing level varies from 600 to 500 m below the mountain crest in the Central Andes and the High Plateau, respectively. No free overpassing level is found in Patagonia. Thus, the impinging flow above the blocking level leads to the streamline collapse on the lee slope.

Figure 9a–c illustrates the dispersion of individual foehn cases around the corresponding composite mean. A constant value of potential temperature is drawn for each individual foehn case in a given region. The thick line represents that value of potential temperature, which coincides with the corresponding isentrope of Fig. 6. The potential temperature value was selected in such a way that isentrope line is positioned above the free overpassing level. Consistently with the previous h diagnostics, upper air from above the blocking level reaches the terrain

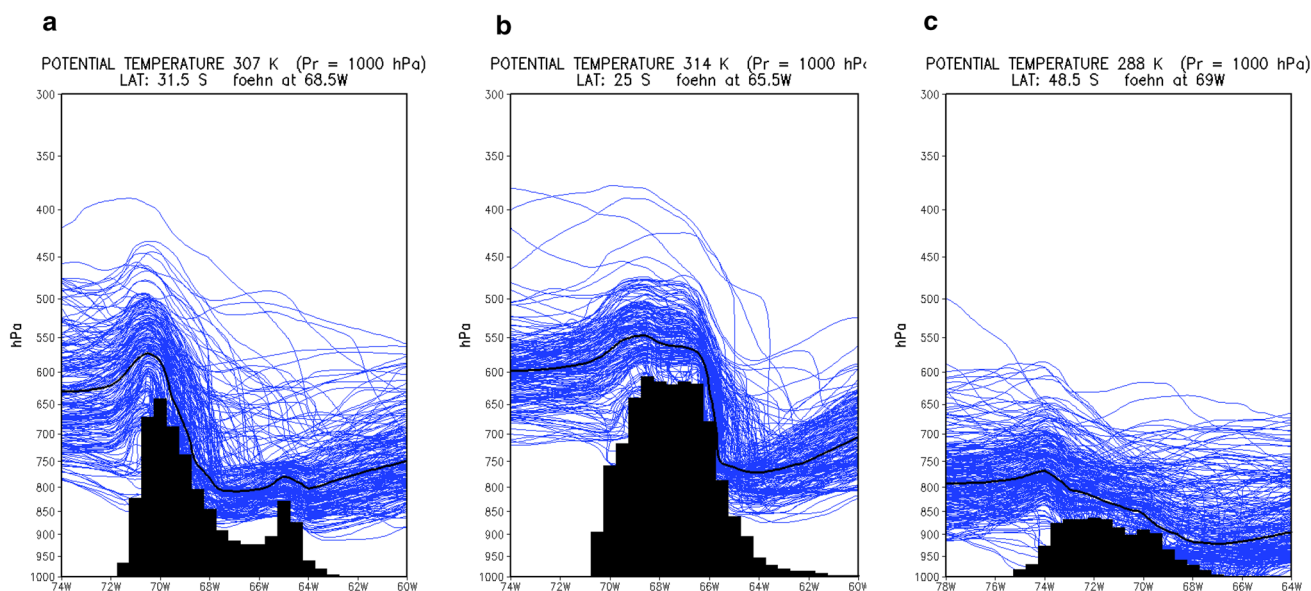


Fig. 9 Vertical cross sections of potential temperature (K) for every foehn case at the Central Andes in July (**a**), the High Plateau in June (**b**) and Patagonia in September (**c**). The thick contour line is the isentrope for the average composite value of 307 K (**a**), 314 K (**b**)

and 288 K (**c**). Thin contour lines are the same isentrope but for each foehn cases. The number of cases in each panel is indicated as n in Table 1

at the longitude where the foehn occurs. In some cases, the descending air originates from a level below the free overpassing level, both in the Central Andes and the High Plateau. This is not the case for Patagonia, where most of the isentropes intersect the terrain even from elevations above the mountain crest level. Few cases of blocked flow seem to occur in the three Andean regions, as seen when the isentropes intersect the windward slopes to the west of the mountain.

To complete the analysis of the vertical structure of the atmosphere, geopotential heights are analyzed at certain pressure levels in Fig. 10. These correspond to the surface pressure of the reference grid point, the mountain crest and a constant pressure of 400 hPa. Cloud covering from the 20-year climate simulation is also shown in the same panels and is classified as low, midlevel, and high clouds.

Left panel of Fig. 10a reveals a weak meridional pressure gradient at foehn level on the eastern slopes of the Central Andes. Low cloud pattern results from the low-level blocking of maritime air to the west of the Andes. At the mountain crest level (middle panel), geopotential height exhibits a strong meridional gradient with a pronounced mountain wave. The sharp edge on the midlevel cloud pattern along the mountain crest is consistent with upslope precipitation (rain and snow) and downwind subsidence. At upperlevels (right panel), the mountain wave persists, which is also evident in the gap of high clouds downwind of the mountain crest.

Geopotential height gradient to the east of the High Plateau at foehn level (Fig. 10b, left panel) corresponds to the weak northwesterly geostrophic wind. Low cloud pattern to the west of the High Plateau reveals the shallow layer of blocked maritime air. At the High Plateau level, the strong meridional geopotential gradient is perturbed by mountain waves (middle panel), which propagate vertically upwards (right panel). Neither midlevel nor high clouds form at the High Plateau latitudes when foehn blows on the eastern slopes. Cloud deck is confined to the south of 27° S and resembles that of the foehn case on the eastern slopes of the Central Andes.

The atmospheric circulation at foehn level over Patagonia (Fig. 10c, left panel) is characterized by a meridional pressure gradient over the entire region and adjacent oceans. A weak trough develops along the Atlantic coast, and a weak ridge along the Pacific coast. Shallow clouds are clustered along the upwind slopes, which is consistent with the orographic lifting of low-level flow. At the crest level (middle panel), geopotential height is characterized by straight lines to the east of the mountain. Midlevel clouds are partially suppressed to the east of the mountain crest. There is no evidence of mountain wave activity or cloud suppression at upperlevels (right panel).

5 Conclusions

Foehn wind is detected in a 20-year regional climate simulation along a broad latitudinal range on the eastern slopes of the Andes. Although the foehn wind is known to blow to the east of the Andes, this is the first time that a comprehensive study shows its regional character to the south of the latitude 15° S. The results show that foehn wind is more frequent to the east of the Central Andes where previous studies investigate zonda wind between the latitudes of 30° S and 35° S (e.g., Norte 1988; Antico et al. 2017).

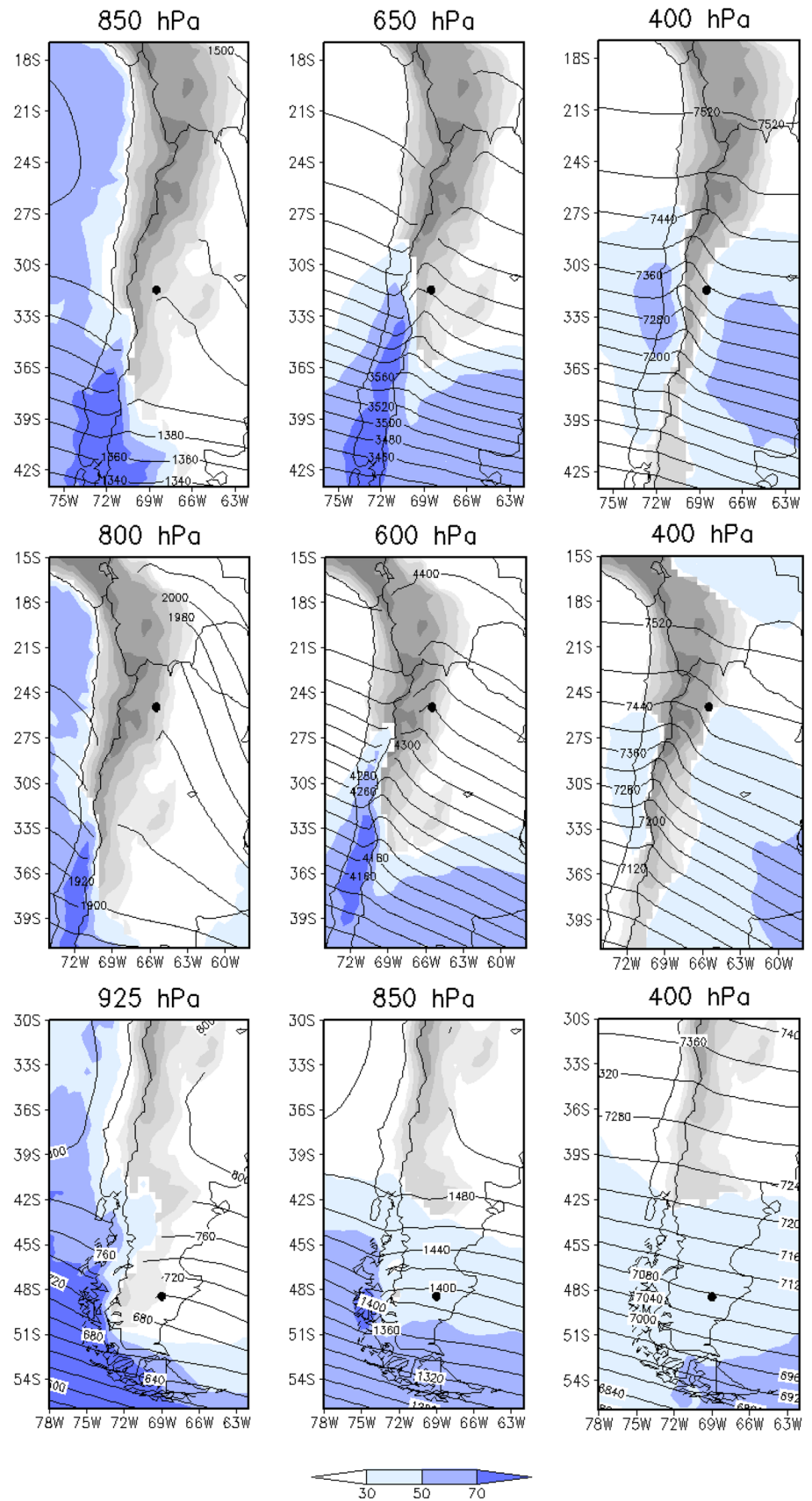
The foehn wind is more frequent during winter in the eastern slopes of the Central Andes and the High Plateau, which agrees with previous results for Mendoza area based on observations (e.g., Norte 1988) and on numerical simulations (Antico et al. 2017). These previous studies found the relative maximum of foehn frequency during spring, which is also evident in our results. Foehn frequency does not exhibit an annual cycle at Patagonia, where it evenly blows at all seasons with weak maximum in September.

Flow blocking occurs when foehn blows on the eastern slopes of the Central Andes and the High Plateau. We defined a blocking level that prevents low-level flow to lift along the upwind slopes of the Andes. Instead, the downslope wind which causes foehn seems to originate from a layer above the blocking level. At the Central Andes, rising air produces rain and snow that may contribute to foehn development.

An intense cross-mountain horizontal gradient of sea level pressure develops when foehn blows on the eastern slopes of the Central Andes and the High Plateau. This gradient results from pressure difference between the high pressure on the Pacific Ocean and the low pressure to the east of the Andes. The resulting sea level pressure pattern is consistent with the low-level flow blocking to the west of the Andes. The low pressure to the east of the Andes is a known feature of the regional circulation when zonda blows at Mendoza (Lichtenstein 1980; Seluchi et al. 2003). Our results show that a similar low pressure also develops when zonda blows on the eastern slopes of the High Plateau.

Foehn is not necessarily in geostrophic balance to the east of the Central Andes and the High Plateau. Mountain wave activity supports this hypothesis together with the cross-mountain pressure gradient at foehn level. This is not the case for Patagonia, where foehn wind is in geostrophic balance. The low-blocking height is consistent with more frequent non-blocked flow. The analysis of individual values of the non-dimensional mountain height (not shown) supports this hypothesis. Because the high frequency of transient synoptic disturbances at Patagonia, sea level pressure commonly fluctuates below and above 1000 hPa.

Fig. 10 Composites of geopotential height (in m) and cloud covering from the 20-year climate simulation. Pressure of the geopotential height corresponds to the reference point level where foehn is detected (left column), the mountain crest level (middle column) and the 400 hPa level (right column) for the Central Andes in July (a), the High Plateau in June (b) and Patagonia in September (c). Cloud covering is represented with shades in light blue as percentages of low clouds (left column), midlevel clouds (middle column) and high clouds (right column). Terrain elevation is shaded for reference



As a result, low-level flow may be blocked or not. In both situations, the flow over the mountains tends to descend downslope. This result is consistent with the permanent foehn effect during the whole year in Patagonia, a known desert region.

The resolution used in the climate simulation is not the most appropriate to represent small-scale circulations. However, results obtained from a 20-year period are consistent enough to make the diagnostics of foehn wind to the east of the Andes at a regional scale. Individual case studies should be investigated in higher spatial and temporal resolutions, in which the effect of physical processes may be investigated in more detail. In all cases, results from observational data are required to validate numerical simulations.

Acknowledgements We are grateful to two anonymous reviewers for their valuable contribution to our work. We thank the editor, Fedor Mesinger, for his suggestions at the time of the manuscript revision. This research was partially supported by Conselho Nacional de Desenvolvimento Científico e Tecnológico grants 306757/2017-6, 400071/2014-2.

Appendix A

Non-dimensional mountain height and blocking diagnosis.

The parameter h as defined by Smith (1988), also known as the inverse Froude number, represents the non-dimensional mountain height. It depends on the mountain height, the wind velocity, and the static stability of the incident flow, as follows:

$$h = \frac{Nh_0}{U},$$

where N is the Brunt–Väisälä frequency, h_0 is the relative height of the mountain crest defined as $Z_{\text{crest}} - Z_0$, where Z_{crest} is the altitude of the mountain crest and Z_0 the altitude of the 1000 hPa pressure level, U is the velocity of the wind perpendicular to the mountain at the crest level.

The bulk method of Reinecke and Durran (2008) is applied to calculate N , as follows:

$$N = \sqrt{\frac{g}{\theta_0} \frac{\theta_{h_0} - \theta_0}{h_0}},$$

where $g = 9.8 \text{ m s}^{-2}$ is the gravity acceleration, θ_0 is the air temperature at the 1000 hPa level upwind of the mountain, and $\theta_{h_0} = T \left(\frac{1000}{p} \right)^{\frac{R}{c_p}}$ is the potential temperature at the crest level upwind of the mountain, where T is the air temperature at the crest level upwind of the mountain, p is the air pressure at the crest level, $R = 287 \text{ J kg}^{-1} \text{ K}^{-1}$ is the gas constant for dry air and $c_p = 1004 \text{ J kg}^{-1} \text{ K}^{-1}$ is the specific heat at constant pressure for dry air.

The theory presented by Smith (1988) estimates conditions under which orographic blocking occurs based on the linear theory for air flow over an isolated mountain. The following conditions are obtained:

| | |
|-----------------------|--|
| $0 < h < \frac{1}{2}$ | Flux overpasses the mountain |
| $h = \frac{1}{2}$ | Streamlines collapse on the lee slope |
| $\frac{1}{2} < h < 1$ | Region of collapsed streamlines spreads to cover more of the lee slope |
| $h = 1$ | Collapsed region reaches the mountain crest |
| $1 < h$ | Windward blocking occurs. Flow may overpass aloft |

References

- Antico PL, Chou SC, Mourão C (2017) Zonda downslope winds in the central Andes of South America in a 20-year climate simulation with the Eta model. *Theor Appl Climatol* 128:291–299. <https://doi.org/10.1007/s00704-015-1709-2>
- Beusch L, Raveh-Rubin S, Sprenger M, Papritz L (2017) Dynamics of a Puelche foehn event in the Andes. *Meteorol Z* 27:67–80. <https://doi.org/10.1127/metz/2017/0841>
- Brinkmann WAR (1971) What is a foehn? *Weather* 26:230–240. <https://doi.org/10.1002/j.1477-8696.1971.tb04200.x>
- Chen F, Janjić ZI, Mitchell K (1997) Impact of atmospheric surface-layer parameterization in the new land-surface scheme of the NCEP mesoscale eta model. *Boundary-Layer Meteorol* 85:391–421
- Dee DP et al (2011) The ERA-Interim reanalysis configuration and performance of the data assimilation system. *Q J R Meteorol Soc* 137:553–597
- Ek MB, Mitchell KE, Lin Y, Rogers E, Grummen P, Koren V, Gayno G, Tarpley JD (2003) Implementation of NOAA land surface advances in the National Centers for Environmental Prediction operational mesoscale Eta model. *J Geophys Res* 108:8851. <https://doi.org/10.1029/2002JD003246>
- Escobar CJE, Seluchi ME (2012) Classificação sinótica dos campos de pressão atmosférica na América do Sul e sua relação com as baixas do Chaco e do noroeste Argentino [Synoptic classification of the atmospheric pressure fields over South America and its relation to the Chaco and the Argentinean northwest lows, T]. *Rev Bras Meteorol* 27:365–375
- Janjić ZI (1990) The step-mountain coordinate: physical package. *Mon Weather Rev* 118(7):1429–1443
- Janjić ZI (1994) The step-mountain eta coordinate model: further developments of the convection, viscous sublayer and turbulence closure schemes. *Mon Weather Rev* 122:927–945
- Janjić ZI (2002) Nonsingular Implementation of the Mellor-Yamada Level 2.5 Scheme in the NCEP Meso Model. NCEP Office Note, 61 p. <https://www.emc.ncep.noaa.gov/officenotes/newernotes/on437.pdf>
- Lichtenstein ER (1980) La Depresión del Noroeste Argentino [The Argentinean northwest low, T]. Universidad de Buenos Aires. PhD dissertation. https://digital.bl.fcen.uba.ar/Download/Tesis/Tesis_1649_Lichtenstein.pdf

- Mellor GL, Yamada T (1982) Development of a turbulence closure model for geophysical fluid problems. *Rev Geophys Space Phys* 20:851–875
- Mesinger F (1993) Forecasting upper tropospheric turbulence within the framework of the Mellor-Yamada 2.5 closure. *Res Act Atmos Ocean Model* 18:4.28–4.29
- Mesinger F (2010) Several PBL parameterization lessons arrived at running an NWP model. In: Intern. conference on planetary boundary layer and climate change, IOP Publishing, IOP Conference Series: Earth and Environmental Science 13. <https://doi.org/10.1088/1755-1315/13/1/012005> (<https://iopscience.iop.org/1755-1315/13/1/012005>)
- Mesinger F, Jovic D (2002) The Eta slope adjustment: contender for an optimal steepening in a piecewise-linear advection scheme? Comparison tests. NCEP Office Note 439. <https://www.emc.ncep.noaa.gov/officenotes>
- Mesinger F, Veljovic K (2017) Eta vs. sigma: review of past results, Gallus-Klemp test, and large-scale wind skill in ensemble experiments. *Meteorol Atmos Phys* 129:573. <https://doi.org/10.1007/s00703-016-0496-3>
- Mesinger F, Wobus RL, Baldwin ME (1996) Parameterization of form drag in the Eta Model at the National Centers for Environmental Prediction. In: 11th conference on numerical weather prediction, Norfolk. Am Meteorol Soc, pp 324–326
- Mesinger F, Chou SC, Gomes JL, Jovic D, Bastos P, Bustamante JF, Lazic L, Lyra AA, Morelli S, Ristic I, Veljovic K (2012) An upgraded version of the Eta model. *Meteorol Atmos Phys* 116:63–79. <https://doi.org/10.1007/s00703-012-0182-z>
- Montecinos A, Muñoz RC, Oviedo S, Martínez A, Villagrán V (2017) Climatological characterization of Puelche winds down the western slope of the extratropical Andes mountains using the NCEP Climate Forecast System Reanalysis. *J Appl Meteorol Clim* 56:677–696. <https://doi.org/10.1175/JAMC-D-16-0289.1>
- Norte FA (1988) Características del Viento Zonda en la Región de Cuyo [Zonda wind features at Cuyo region, T]. University of Buenos Aires, PhD dissertation. https://digital.bl.fcen.uba.ar/Download/Tesis/Tesis_2131_Norte.pdf
- Norte FA (2015) Understanding and forecasting Zonda wind (Andean Foehn) in Argentina: a review. *Atmos Clim Sci* 5:163–193
- Norte FA, Ulke AG, Simonelli SC, Viale M (2008) The severe zonda wind event of 11 July 2006 east of the Andes Cordillera (Argentina): a case study using the BRAMS model. *Meteorol Atmos Phys* 102:1–14
- Puliafito SE, Allende DG, Mulena CG, Cremades P, Lakkis SG (2015) Evaluation of the WRF model configuration for Zonda wind events in a complex terrain. *Atmos Res* 166:24–32. <https://doi.org/10.1016/j.atmosres.2015.06.011>
- Reinecke PA, Durran DR (2008) Estimating topographic blocking using a Froude number when static stability is nonuniform. *J Atmos Sci* 65:1035–1048. <https://doi.org/10.1175/2007JAS2100.1>
- Rutllant J, Garreaud R (2004) Episodes of Strong Flow down the Western Slope of the Subtropical Andes. *Mon Weather Rev* 132:611–622. [https://doi.org/10.1175/1520-0493\(2004\)132<0611:EOSFD T>2.0.CO;2](https://doi.org/10.1175/1520-0493(2004)132<0611:EOSFD T>2.0.CO;2)
- Schwerdtfeger W (1976) Climates of Central and South America. In: Landsberg HE (ed) *World Survey of Climatology*. Elsevier, Amsterdam, pp 13–112
- Seluchi ME, Norte FA, Satyamurty P, Chou SC (2003) Analysis of three situations of the Foehn effect over the Andes (Zonda wind) using the Eta-CPTEC regional model. *Weather Forecast* 18:481–501
- Smith RB (1988) Linear theory of stratified flow past an isolated mountain in isosteric coordinates. *J Atmos Sci* 45:3889–3896
- Würsch M, Sprenger M (2015) Swiss and Austrian foehn revisited: a Lagrangian-based analysis. *Meteorol Z* 24:225–242. <https://doi.org/10.1127/metz/2015/0647>
- Zhao Q, Black TL, Baldwin ME (1997) Implementation of the cloud prediction scheme in the Eta model at NCEP. *Weather Forecast* 12:697–712
- Zilitinkevich SS (1995) Non-local turbulent transport: Pollution dispersion aspects of coherent structure of convective flows. In: Power H, Moussiopoulos N, Brebbia CA (eds) *Air pollution III. Air pollution theory and simulation, vol I. Computational Mechanics Publications, Southampton*, pp 53–60

Publisher's Note Springer Nature remains neutral with regard to jurisdictional claims in published maps and institutional affiliations.